

Q^2 -evolution of parton densities at small- x values

A.Yu. Illarionov¹ and A.V. Kotikov²

¹*Dipartimento di Fisica dell'Università di Trento,*

via Sommarive 14, I-38050 Povo, Trento, Italy.

E-mail: illario@science.unitn.it

²*Joint Institute for Nuclear Research, Dubna, Russia.*

E-mail: kotikov@theor.jinr.ru

In the leading twist approximation of the Wilson operator product expansion with “frozen” and analytic strong coupling constants we show that Bessel-inspired behavior of the structure function F_2 at small x , obtained for a flat initial condition in the DGLAP evolution equations, leads to good agreement with the deep inelastic scattering experimental data from HERA.

PACS numbers: 13.60.Hb, 12.38.Bx

I. INTRODUCTION

The experimental data from HERA on the deep-inelastic scattering (DIS) structure function (SF) F_2 [1, 2], and its derivatives $\partial F_2 / \partial \ln(Q^2)$ [1, 3] and $\partial \ln F_2 / \partial \ln(1/x)$ [3, 4, 5] enter us into a very interesting kinematical range for testing the theoretical ideas on the behavior of quarks and gluons carrying a very low fraction of momentum of the proton, the so-called small- x region. In this limit one expects that the conventional treatment based on the Dokshitzer–Gribov–Lipatov–Altarelli–Parisi (DGLAP) equations does not account for contributions to the cross section which are leading in $\alpha_s \ln(1/x)$ and, moreover, the parton densities (PD), in particular the gluons, are becoming large and need to develop a high density formulation of QCD.

However, the reasonable agreement between HERA data and the next-to-leading-order (NLO) approximation of perturbative QCD has been observed for $Q^2 \geq 2 \text{ GeV}^2$ (see reviews in [6] and references therein) and, thus, perturbative QCD could describe the evolution of F_2 and its derivatives up to very low Q^2 values, traditionally explained by soft processes.

The standard program to study the x behavior of quarks and gluons is carried out by

comparison of data with the numerical solution of the DGLAP equations [7]¹ by fitting the parameters of the x -profile of partons at some initial Q_0^2 and the QCD energy scale Λ [9, 10, 11]. However, for analyzing exclusively the small- x region, there is the alternative of doing a simpler analysis by using some of the existing analytical solutions of DGLAP in the small- x limit [12]–[15]. This was done so in [12] where it was pointed out that the HERA small- x data can be interpreted in terms of the so-called doubled asymptotic scaling (DAS) phenomenon related to the asymptotic behavior of the DGLAP evolution discovered many years ago [16].

The study of [12] was extended in [13, 14, 15] to include the finite parts of anomalous dimensions of Wilson operators and Wilson coefficients². This has led to predictions [14, 15] of the small- x asymptotic PD form in the framework of the DGLAP dynamics starting at some Q_0^2 with the flat function

$$f_a(Q_0^2) = A_a \quad (\text{hereafter } a = q, g), \quad (1)$$

where f_a are the parton distributions multiplied by x and A_a are unknown parameters to be determined from the data.

We refer to the approach of [13, 14, 15] as *generalized* DAS approximation. In the approach the flat initial conditions in Eq. (1) determine the basic role of the singular parts of anomalous dimensions, as in the standard DAS case, while the contribution from finite parts of anomalous dimensions and from Wilson coefficients can be considered as corrections which are, however, important for better agreement with experimental data. In the present paper, similar to [12]–[15], we neglect the contribution from the non-singlet quark component.

The use of the flat initial condition given in Eq. (1) is supported by the actual experimental situation: low- Q^2 data [1, 3, 17, 18] are well described for $Q^2 \leq 0.4 \text{ GeV}^2$ by Regge theory with Pomeron intercept $\alpha_P(0) \equiv \lambda_P + 1 = 1.08$, closed to the standard ($\alpha_P(0) = 1$) one. The small rise of HERA data [1, 3, 18, 19] at low Q^2 can be explained, for example, by contributions of higher twist operators (see [15]).

The purpose of this paper is to demonstrate a good agreement between the predictions

¹ At small x there is another approach based on the Balitsky–Fadin–Kuraev–Lipatov (BFKL) equation [8], whose application is out of the scope of this work.

² In the standard DAS approximation [16] only the singular parts of the anomalous dimensions were used.

from the generalized DAS approach and the HERA experimental data [1, 2] (see Figs. 1–3) for SF F_2 and also to compare the predictions for the slope $\partial \ln F_2 / \partial \ln(1/x)$ with the H1 and ZEUS data [3, 4, 5]. Looking at the H1 data [1] points shown in Figs. 4 and 5 one can conclude that $\lambda(Q^2)$ is independent on x within the experimental uncertainties for fixed Q^2 in the range $x < 0.01$. Indeed, the data are well described by the power behavior

$$F_2(x, Q^2) = Cx^{-\lambda(Q^2)}, \quad (2)$$

where $\lambda(Q^2) = \hat{a} \ln(Q^2/\Lambda^2)$ with $C \approx 0.18$, $\hat{a} \approx 0.048$ and $\Lambda = 292$ MeV [4]. The linear rise of the exponent $\lambda(Q^2)$ with $\ln Q^2$ is also explicitly shown in Figs. 4 and 5 by the dashed line.

The rise of $\lambda(Q^2)$ linearly with $\ln Q^2$ can be traced in strong nonperturbative way (see [20] and references therein), i.e., $\lambda(Q^2) \sim 1/\alpha_s(Q^2)$. The previous analysis [21], however, demonstrated that the rise can be explained naturally in the framework of perturbative QCD.

The ZEUS and H1 Collaborations have also presented [3, 5] new preliminary data for $\lambda(Q^2)$ at quite low values of Q^2 . As it is possible to see in Fig. 8 of [3], the ZEUS value for $\lambda(Q^2)$ is consistent with a constant ~ 0.1 at $Q^2 < 0.6$ GeV², as it is expected under the assumption of single soft Pomeron exchange within the framework of Regge phenomenology. These points lie slightly below the corresponding ZEUS data but all the results are in agreement within modern experimental errors.

It is important to extend the analysis of [21] to low Q^2 range with a help of well-known infrared modifications of the strong coupling constant. We will use the “frozen” and analytic versions (see, [22] and [23], respectively).

The paper is organized as follows. Section 2 contains basic formulae, which are needed for the present study and were previously obtained in [14, 15, 21]. In Section 3 we compare our calculations with H1 and ZEUS experimental data and present the obtained results. Some discussions can be found in Conclusions.

II. GENERALIZED DAS APPROACH

The flat initial condition (1) corresponds to the case when parton distributions tend to

some constant value at $x \rightarrow 0$ and at some initial value Q_0^2 . The main ingredients of the results [14, 15], are:

- Both, the gluon and quark singlet densities are presented in terms of two components (" + " and " - ") which are obtained from the analytic Q^2 -dependent expressions of the corresponding (" + " and " - ") PD moments.
- The twist-two part of the " - " component is constant at small x at any values of Q^2 , whereas the one of the " + " component grows at $Q^2 \geq Q_0^2$ as

$$\sim e^\sigma, \quad \sigma = 2\sqrt{\left[\hat{d}_+ s - \left(\hat{D}_+ + \hat{d}_+ \frac{\beta_1}{\beta_0}\right)p\right] \ln\left(\frac{1}{x}\right)}, \quad \rho = \frac{\sigma}{2 \ln(1/x)}, \quad (3)$$

where σ and ρ are the generalized Ball-Forte variables,

$$s = \ln\left(\frac{a_s(Q_0^2)}{a_s(Q^2)}\right), \quad p = a_s(Q_0^2) - a_s(Q^2), \quad \hat{d}_+ = \frac{12}{\beta_0}, \quad \hat{D}_+ = \frac{412}{27\beta_0}. \quad (4)$$

Hereafter we use the notation $a_s = \alpha_s/(4\pi)$. The first two coefficients of the QCD β -function in the $\overline{\text{MS}}$ -scheme are $\beta_0 = 11 - (2/3)f$ and $\beta_1 = 102 - (114/9)f$ with f is being the number of active quark flavors.

Note here that the perturbative coupling constant $a_s(Q^2)$ is different at the leading-order (LO) and NLO approximations. Indeed, from the renormalization group equation we can obtain the following equations for the coupling constant

$$\frac{1}{a_s(Q^2)} = \beta_0 \ln\left(\frac{Q^2}{\Lambda_{\text{LO}}^2}\right) \quad (5)$$

at the LO approximation and

$$\frac{1}{a_s(Q^2)} + \frac{\beta_1}{\beta_0} \ln\left[\frac{\beta_0^2 a_s(Q^2)}{\beta_0 + \beta_1 a_s(Q^2)}\right] = \beta_0 \ln\left(\frac{Q^2}{\Lambda^2}\right) \quad (6)$$

at the NLO approximation. Usually at the NLO level $\overline{\text{MS}}$ -scheme is used, so we apply $\Lambda = \Lambda_{\overline{\text{MS}}}$ below.

A. Parton distributions and the structure function F_2

Here, for simplicity we consider only the LO approximation³. The results for parton densities and F_2 are following:

³ The NLO results may be found in [14, 15].

- The structure function F_2 has the form

$$\begin{aligned} F_2(x, Q^2) &= e f_q(x, Q^2), \\ f_a(x, Q^2) &= f_a^+(x, Q^2) + f_a^-(x, Q^2), \end{aligned} \quad (7)$$

where $e = (\sum_1^f e_i^2)/f$ is the average charge square.

- The small- x asymptotic results for PD f_a^\pm are

$$f_g^+(x, Q^2) = \left(A_g + \frac{4}{9}A_q\right) \tilde{I}_0(\sigma) e^{-\bar{d}_+(1)s} + O(\rho), \quad (8)$$

$$f_q^+(x, Q^2) = \frac{f}{9} \left(A_g + \frac{4}{9}A_q\right) \rho \tilde{I}_1(\sigma) e^{-\bar{d}_+(1)s} + O(\rho), \quad (9)$$

$$f_g^-(x, Q^2) = -\frac{4}{9}A_q e^{-d_-(1)s} + O(x), \quad (10)$$

$$f_q^-(x, Q^2) = A_q e^{-d_-(1)s} + O(x), \quad (11)$$

where $\bar{d}_+(1) = 1 + 20f/(27\beta_0)$ and $d_-(1) = 16f/(27\beta_0)$ are the regular parts of the anomalous dimensions $d_+(n)$ and $d_-(n)$, respectively, in the limit $n \rightarrow 1^4$. Here n is the variable in Mellin space. The functions \tilde{I}_ν ($\nu = 0, 1$) are related to the modified Bessel function I_ν and to the Bessel function J_ν by:

$$\tilde{I}_\nu(\sigma) = \begin{cases} I_\nu(\sigma), & \text{if } s \geq 0 \\ i^{-\nu} J_\nu(i\sigma), \quad i^2 = -1, & \text{if } s \leq 0 \end{cases}. \quad (12)$$

At the LO, the variables σ and ρ are given by Eq. (3) when $p = 0$.

B. Effective slopes

Contrary to the approach in [12, 13, 14, 15] various groups have been able to fit the available data using a hard input at small x : $x^{-\lambda}$, $\lambda > 0$ with different λ values at low and high Q^2 (see [24, 25, 26, 27, 28, 29]). Such results are well-known at low Q^2 values [25]. At large Q^2 values, for the modern HERA data it is also not very surprising, because they cannot distinguish between the behavior based on a steep input parton parameterization, at quite large Q^2 , and the steep form acquired after the dynamical evolution from a flat initial condition at quite low Q^2 values.

⁴ We denote the singular and regular parts of a given quantity $k(n)$ in the limit $n \rightarrow 1$ by $\hat{k}(n)$ and $\bar{k}(n)$, respectively.

As it has been mentioned above and shown in [14, 15], the behavior of parton densities and F_2 given in the Bessel-like form by generalized DAS approach can mimic a power law shape over a limited region of x and Q^2

$$f_a(x, Q^2) \sim x^{-\lambda_a^{\text{eff}}(x, Q^2)} \quad \text{and} \quad F_2(x, Q^2) \sim x^{-\lambda_{F_2}^{\text{eff}}(x, Q^2)}.$$

The effective slopes $\lambda_a^{\text{eff}}(x, Q^2)$ and $\lambda_{F_2}^{\text{eff}}(x, Q^2)$ have the form:

$$\begin{aligned} \lambda_g^{\text{eff}}(x, Q^2) &= \frac{f_g^+(x, Q^2)}{f_g(x, Q^2)} \rho \frac{\tilde{I}_1(\sigma)}{\tilde{I}_0(\sigma)}, \\ \lambda_q^{\text{eff}}(x, Q^2) &= \frac{f_q^+(x, Q^2)}{f_q(x, Q^2)} \rho \frac{\tilde{I}_2(\sigma)(1 - 20a_s(Q^2)) + 20a_s(Q^2)\tilde{I}_1(\sigma)/\rho}{\tilde{I}_1(\sigma)(1 - 20a_s(Q^2)) + 20a_s(Q^2)\tilde{I}_0(\sigma)/\rho}, \\ \lambda_{F_2}^{\text{eff}}(x, Q^2) &= \frac{\lambda_q^{\text{eff}}(x, Q^2) f_q^+(x, Q^2) + (2f)/3a_s(Q^2) \lambda_g^{\text{eff}}(x, Q^2) f_g^+(x, Q^2)}{f_q(x, Q^2) + (2f)/3a_s(Q^2) f_g(x, Q^2)}, \end{aligned} \quad (13)$$

where the exact form of parton densities can be found in [14, 15].

The results (13) (and also (14)–(16) below) are given at the NLO approximation. To obtain the LO one, it is necessary to cancel the term $\sim a_s(Q^2)$ and to use Eqs. (8)–(11) for parton densities $f_a(x, Q^2)$.

The effective slopes λ_a^{eff} and $\lambda_{F_2}^{\text{eff}}$ depend on the magnitudes A_a of the initial PD and also on the chosen input values of Q_0^2 and Λ . To compare with the experimental data it is necessary the exact expressions (13), but for qualitative analysis it is better to use an approximation.

C. Asymptotic form of the effective slopes

At quite large values of Q^2 , where the “–” component is negligible, the dependence on the initial PD disappears, having in this case for the asymptotic behavior the following expressions⁵:

$$\lambda_g^{\text{eff,as}}(x, Q^2) = \rho \frac{\tilde{I}_1(\sigma)}{\tilde{I}_0(\sigma)} \approx \rho - \frac{1}{4 \ln(1/x)}, \quad (14)$$

⁵ The asymptotic formulae given in Eqs. (14)–(16) work quite well at any $Q^2 \geq Q_0^2$ values, because at $Q^2 = Q_0^2$ the values of λ_a^{eff} and $\lambda_{F_2}^{\text{eff}}$ are equal zero. The use of approximations in Eqs. (14)–(16) instead of the exact results given in Eq. (13) underestimates (overestimates) only slightly the gluon (quark) slope at $Q^2 \geq Q_0^2$.

$$\begin{aligned}\lambda_q^{\text{eff,as}}(x, Q^2) &= \rho \frac{\tilde{I}_2(\sigma)(1 - 20a_s(Q^2)) + 20a_s(Q^2)\tilde{I}_1(\sigma)/\rho}{\tilde{I}_1(\sigma)(1 - 20a_s(Q^2)) + 20a_s(Q^2)\tilde{I}_0(\sigma)/\rho} \\ &\approx \rho - \frac{3}{4 \ln(1/x)} + \frac{10a_s(Q^2)}{\rho \ln(1/x)},\end{aligned}\quad (15)$$

$$\begin{aligned}\lambda_{F_2}^{\text{eff,as}}(x, Q^2) &= \rho \frac{\tilde{I}_2(\sigma)}{\tilde{I}_1(\sigma)} + 26a_s(Q^2) \left(1 - \frac{\tilde{I}_0(\sigma)\tilde{I}_2(\sigma)}{\tilde{I}_1^2(\sigma)}\right) \\ &\approx \rho - \frac{3}{4 \ln(1/x)} + \frac{13a_s(Q^2)}{\rho \ln(1/x)} = \lambda_q^{\text{eff,as}}(x, Q^2) + \frac{3a_s(Q^2)}{\rho \ln(1/x)},\end{aligned}\quad (16)$$

where the symbol \approx marks the approximation obtained in the expansion of the usual and modified Bessel functions in (12). These approximations are accurate only at very large σ values (i.e. at very large Q^2 and/or very small x).

As one can see from Eqs. (14) and (15), the gluon effective slope λ_g^{eff} is larger than the quark slope λ_q^{eff} , which is in excellent agreement with MRS [30] and GRV [10] analyses (see also [9]).

We would like to note that at the NLO approximation the slope $\lambda_{F_2}^{\text{eff,as}}(x, Q^2)$ lies between quark and gluon ones but closely to quark slope $\lambda_q^{\text{eff,as}}(x, Q^2)$. Indeed,

$$\lambda_g^{\text{eff,as}}(x, Q^2) - \lambda_{F_2}^{\text{eff,as}}(x, Q^2) \approx \left(\rho - \frac{1}{4 \ln(1/x)} + 26a_s(Q^2)\right) \frac{1}{2\rho \ln(1/x)}, \quad (17)$$

$$\lambda_{F_2}^{\text{eff,as}}(x, Q^2) - \lambda_q^{\text{eff,as}}(x, Q^2) \approx \frac{3a_s(Q^2)}{\rho \ln(1/x)}. \quad (18)$$

Both slopes $\lambda_a^{\text{eff}}(x, Q^2)$ decrease with increasing x (see Fig. 5). A x -dependence of the slope should not appear for a PD within a Regge type asymptotic ($x^{-\lambda}$) and precise measurement of the slope $\lambda_a^{\text{eff}}(x, Q^2)$ may lead to the possibility to verify the type of small- x asymptotics of parton distributions.

III. COMPARISON WITH EXPERIMENTAL DATA

Using the results of previous section we have analyzed HERA data for F_2 and the slope $\partial \ln F_2 / \partial \ln(1/x)$ at small x from the H1 and ZEUS Collaborations [1, 2, 3, 4, 5].

In order to keep the analysis as simple as possible, we fix $f = 4$ and $\alpha_s(M_Z^2) = 0.1166$ (i.e., $\Lambda^{(4)} = 284$ MeV) in agreement with the more recent ZEUS results [2].

As it is possible to see in Figs. 1–3 (see also [14, 15]), the twist-two approximation is reasonable at $Q^2 \geq 2$ GeV². At smaller Q^2 , some modification of the approximation should

be considered. In the recent article [15] we have added the higher twist corrections. For renormalon model of higher twists, we have found a good agreement with experimental data at essentially lower Q^2 values: $Q^2 \geq 0.5 \text{ GeV}^2$ (see Figs. 2 and 3).

Moreover, the results of fits in [15] have an important property: they are very similar in LO and NLO approximations of perturbation theory. The similarity is related to the fact that the small- x asymptotics of the NLO corrections are usually large and negative (see, for example, α_s -corrections [31] to BFKL kernel [8]⁶). Then, the LO form $\sim \alpha_s(Q^2)$ for some observable and the NLO one $\sim \alpha_s(Q^2)(1 - K\alpha_s(Q^2))$ with a large value of K are similar, because $\Lambda \gg \Lambda_{\text{LO}}$ ⁷ and, thus, $\alpha_s(Q^2)$ at LO is considerably smaller than $\alpha_s(Q^2)$ at NLO for HERA Q^2 values.

In other words, performing some resummation procedure (such as Grunberg's effective-charge method [32]), one can see that the NLO form may be represented as $\sim \alpha_s(Q_{\text{eff}}^2)$, where $Q_{\text{eff}}^2 \gg Q^2$. Indeed, from different studies [33, 34, 35], it is well known that at small- x values the effective argument of the coupling constant is higher than Q^2 .

Here, to improve the agreement at small Q^2 values, we modify the QCD coupling constant. We consider two modifications, which effectively increase the argument of the coupling constant at small Q^2 values (in agreement with [33, 34, 35]).

In one case, which is more phenomenological, we introduce freezing of the coupling constant by changing its argument $Q^2 \rightarrow Q^2 + M_\rho^2$, where M_ρ is the ρ -meson mass (see [22]). Thus, in the formulae of the Section 2 we should do the following replacement:

$$a_s(Q^2) \rightarrow a_{\text{fr}}(Q^2) \equiv a_s(Q^2 + M_\rho^2) \quad (19)$$

The second possibility incorporates the Shirkov–Solovtsov idea [23, 36, 37] about analyticity of the coupling constant that leads to the additional its power dependence. Then, in the formulae of the previous section the coupling constant $a_s(Q^2)$ should be replaced as follows:

$$a_{\text{an}}^{\text{LO}}(Q^2) = a_s(Q^2) - \frac{1}{\beta_0} \frac{\Lambda_{\text{LO}}^2}{Q^2 - \Lambda_{\text{LO}}^2} \quad (20)$$

⁶ It seems that it is a property of any processes in which gluons, but not quarks play a basic role.

⁷ The equality of $\alpha_s(M_Z^2)$ at LO and NLO approximations, where M_Z is the Z -boson mass, relates Λ and Λ_{LO} : $\Lambda^{(4)} = 284 \text{ MeV}$ (as in [2]) corresponds to $\Lambda_{\text{LO}} = 112 \text{ MeV}$ (see [15]).

at the LO approximation and

$$a_{\text{an}}(Q^2) = a_s(Q^2) - \frac{1}{2\beta_0} \frac{\Lambda^2}{Q^2 - \Lambda^2} + \dots, \quad (21)$$

at the NLO approximation, where the symbol \dots stands for terms which have negligible contributions at $Q \geq 1$ GeV [23]⁸.

Figure 4 shows the experimental data for $\lambda_{F_2}^{\text{eff}}(x, Q^2)$ ⁹ at $x \sim 10^{-3}$, which represents an average of the x -values of HERA experimental data. The top dashed line represents the aforementioned linear rise of $\lambda(Q^2)$ with $\ln(Q^2)$.

Figure 4 demonstrates that the theoretical description of the small- Q^2 ZEUS data for $\lambda_{F_2}^{\text{eff}}(x, Q^2)$ by NLO QCD is significantly improved by implementing the “frozen” and analytic coupling constants $\alpha_{\text{fr}}(Q^2)$ and $\alpha_{\text{an}}(Q^2)$, respectively, which in turn lead to very close results (see also [39]).

Indeed, the fits for $F_2(x, Q^2)$ in [15] yielded $Q_0^2 \approx 0.5\text{--}0.8$ GeV². So, initially we had $\lambda_{F_2}^{\text{eff}}(x, Q_0^2) = 0$, as suggested by Eq. (1). The replacements of Eqs. (19), (20) and (21) modify the value of $\lambda_{F_2}^{\text{eff}}(x, Q_0^2)$. For the “frozen” and analytic coupling constants $\alpha_{\text{fr}}(Q^2)$ and $\alpha_{\text{an}}(Q^2)$, the value of $\lambda_{F_2}^{\text{eff}}(x, Q_0^2)$ is nonzero and the slopes are quite close to the experimental data at $Q^2 \approx 0.5$ GeV². Nevertheless, for $Q^2 \leq 0.5$ GeV², there is still some disagreement with the data, which needs additional investigation.

Figure 5 shows the x -dependence of the slope $\lambda_{F_2}^{\text{eff}}(x, Q^2)$. One observes good agreement between the experimental data and the generalized DAS approach for a broad range of small- x values. The absence of a variation with x of $\lambda_{F_2}^{\text{eff}}(x, Q^2)$ at small Q^2 values is related to the small values of the variable ρ there.

At large Q^2 values, the x -dependence of $\lambda_{F_2}^{\text{eff}}(x, Q^2)$ is rather strong. However, it is well known that the boundaries and mean values of the experimental x ranges [4] increase proportionally with Q^2 , which is related to the kinematical restrictions in the HERA experiments: $x \sim 10^{-4} \times Q^2$ (see [1, 2, 21] and, for example, Fig. 1 of [3]). We show only the case with the “frozen” coupling constant because at large Q^2 values all results are very similar.

⁸ Note that in [36, 37] more accurate, but essentially more cumbersome approximations of $a_{\text{an}}(Q^2)$ have been proposed. We limit ourselves by above simple form (20), (21) and plan to add the other modifications in our future investigations.

⁹ Using the “frozen” and analytic coupling constants, the experimental data for $F_2(x, Q^2)$ have been analysed recently in [38].

From Fig. 5, one can see that HERA experimental data are close to $\lambda_{F_2}^{\text{eff}}(x, Q^2)$ at $x \sim 10^{-4} \div 10^{-5}$ for $Q^2 = 4 \text{ GeV}^2$ and at $x \sim 10^{-2}$ for $Q^2 = 100 \text{ GeV}^2$. Indeed, the correlations between x and Q^2 in the form $x_{\text{eff}} = a \times 10^{-4} \times Q^2$ with $a = 0.1$ and 1 lead to a modification of the Q^2 evolution which starts to resemble $\ln Q^2$, rather than $\ln \ln Q^2$ as is standard [21].

IV. CONCLUSIONS

We shown the Q^2 -dependence of the structure function F_2 and the slope $\lambda_{F_2}^{\text{eff}} = \partial \ln F_2 / \partial \ln(1/x)$ at small- x values in the framework of perturbative QCD. Our twist-two results are in very good agreement with precise HERA data at $Q^2 \geq 2 \text{ GeV}^2$, where perturbative theory can be applicable. The application of the “frozen” and analytic coupling constants $\alpha_{\text{fr}}(Q^2)$ and $\alpha_{\text{an}}(Q^2)$ improves the agreement with the recent HERA data [3, 4, 5] for the slope $\lambda_{F_2}^{\text{eff}}(x, Q^2)$ for small Q^2 values, $Q^2 \geq 0.5 \text{ GeV}^2$.

As a next step of investigations, we plan to fit the HERA data [1, 2, 3, 4, 5] of $F_2(x, Q^2)$ directly, using the “frozen” and analytic coupling constants in both the LO and NLO approximations, in order to improve the agreement with HERA data at small Q^2 values. Several versions of the analytical coupling constant will be used.

This work was supported by RFBR grant 07-02-01046-a. A.V.K. thanks the Organizing Committee of Workshop on Physics of Fundamental Interactions for invitation.

-
- [1] H1 Collab. (C. Adloff *et al.*), Nucl. Phys. B **497**, 3 (1997); Eur. Phys. J. C **21**, 33 (2001).
 - [2] ZEUS Collab. (S. Chekanov *et al.*), Eur. Phys. J. C **21**, 443 (2001).
 - [3] ZEUS Collab. (B. Surrow), hep-ph/0201025.
 - [4] H1 Collab. (C. Adloff *et al.*), Phys. Lett. B **520**, 183 (2001).
 - [5] H1 Collab. (T. Lastovicka), Acta Phys. Polon. B **33**, 2835 (2002); H1 Collab. (J. Gayler), Acta Phys. Polon. B **33**, 2841 (2002).
 - [6] A. M. Cooper-Sarkar, R. C. E. Devenish, and A. De Roeck, Int. J. Mod. Phys. A **13**, 3385 (1998); A. V. Kotikov, Phys. Part. Nucl. **38**, 1, 828 (Erratum) (2007).

- [7] V. N. Gribov and L. N. Lipatov, Sov. J. Nucl. Phys. **15**, 438, 675 (1972); L. N. Lipatov, Sov. J. Nucl. Phys. **20**, 94 (1975); G. Altarelli and G. Parisi, Nucl. Phys. B **126**, 298 (1977); Yu. L. Dokshitzer, Sov. Phys. JETP **46**, 641 (1977).
- [8] L. N. Lipatov, Sov. J. Nucl. Phys. **23**, 338 (1976); E. A. Kuraev, L. N. Lipatov, and V. S. Fadin, Phys. Lett. B **60**, 50 (1975); Sov. Phys. JETP **44**, 443 (1976); **45**, 199 (1977); Ya. Ya. Balitzki and L. N. Lipatov, Sov. J. Nucl. Phys. **28**, 822 (1978); L. N. Lipatov, Sov. Phys. JETP **63**, 904 (1986).
- [9] A. D. Martin and W. S. Stirling, R.G. Roberts, R.S. Thorne, Eur. Phys. J. C **23**, 73 (2002); J. Pumplin *et al.* (CTEQ Collab.), JHEP **0207**, 012 (2002); JHEP **0602**, 032 (2006).
- [10] M. Gluck, E. Reya, and A. Vogt, Eur. Phys. J. C **5**, 461 (1998); M. Gluck, C. Pisano, and E. Reya, Eur. Phys. J. C **40**, 515 (2005).
- [11] A. V. Kotikov, G. Parente, and J. Sanchez Guillen, Z. Phys. C **58**, 465 (1993); G. Parente, A. V. Kotikov, and V. G. Krivokhizhin, Phys. Lett. B **333**, 190 (1994); A. L. Kataev, A. V. Kotikov, G. Parente, and A. V. Sidorov, Phys. Lett. B **388**, 179 (1996); Phys. Lett. B **417**, 374 (1998); A. L. Kataev, G. Parente, and A. V. Sidorov, Nucl. Phys. B **573**, 405 (2000); A. V. Kotikov and V. G. Krivokhijine, Phys. At. Nucl. **68**, 1873 (2005) (hep-ph/0108224).
- [12] R. D. Ball and S. Forte, Phys. Lett. B **336**, 77 (1994).
- [13] L. Mankiewicz, A. Saalfeld, and T. Weigl, Phys. Lett. B **393**, 175 (1997).
- [14] A. V. Kotikov and G. Parente, Nucl. Phys. B **549**, 242 (1999); Nucl. Phys. (Proc. Suppl.) A **99**, 196 (2001).
- [15] A. Yu. Illarionov, A. V. Kotikov, and G. Parente, Phys. Part. Nucl. **39**, 307 (2008); Nucl. Phys. (Proc. Suppl.) **146**, 234 (2005).
- [16] A. De Rújula, S. L. Glashow, H. D. Politzer *et. al.*, Phys. Rev. D **10**, 1649 (1974).
- [17] NM Collab. (M. Arneodo *et al.*), Phys. Lett. B **364**, 107 (1995); Nucl. Phys. B **483**, 3 (1997); E665 Collab. (M. R. Adams *et al.*), Phys. Rev. D **54**, 3006 (1996); A. Donnachie and P. V. Landshoff, Nucl. Phys. B **244**, 322 (1984); **267**, 690 (1986); Z. Phys. C **61**, 139 (1994).
- [18] ZEUS Collab. (J. Breitweg *et al.*), Phys. Lett. B **407**, 432 (1997).
- [19] ZEUS Collab. (J. Breitweg *et al.*), Phys. Lett. B **487**, 53 (2000); Eur. Phys. J. C **21**, 443 (2001).
- [20] F. Schrempp, hep-ph/0507160.
- [21] A. V. Kotikov and G. Parente, J. Exp. Theor. Phys. **97**, 859 (2003).

- [22] G. Curci, M. Greco, and Y. Srivastava, Phys. Rev. Lett. **43**, 834 (1979); Nucl. Phys. B **159**, 451 (1979); M. Greco, G. Penso, and Y. Srivastava, Phys. Rev. D **21**, 2520 (1980); PLUTO Collab.(C. Berger *et al.*), Phys. Lett. B **100**, 351 (1981); N. N. Nikolaev and B. M. Zakharov, Z. Phys. C **49**, 607 (1991); **53**, 331 (1992); B. Badelek, J. Kwiecinski, and A. Stasto, Z. Phys. C **74**, 297 (1997).
- [23] D. V. Shirkov and I. L. Solovtsov, Phys. Rev. Lett **79**, 1209 (1997); Theor. Math. Phys. **120**, 1220 (1999).
- [24] C. Lopez and F. J. Ynduráin, Nucl. Phys. B **171**, 231 (1980); Nucl. Phys. B **183**, 157 (1981); C. Lopez, F. Barreiro, and F. J. Ynduráin, Z. Phys. C **72**, 561 (1996); K. Adel, F. Barreiro, and F. J. Ynduráin, Nucl. Phys. B **495**, 221 (1997).
- [25] A. Donnachie and P. V. Landshoff, Phys. Lett. B **296**, 227 (1992); Phys. Lett. B **437**, 408 (1998).
- [26] H. Abramowitz, E. M. Levin, A. Levy, and U. Maor, Phys. Lett. B **269**, 465 (1991); A. V. Kotikov, Mod. Phys. Lett. A **11**, 103 (1996); Phys. At. Nucl. **59**, 2137 (1996).
- [27] A. V. Kotikov, Phys. At. Nucl. **56**, 1276 (1993); **57**, 133 (1994); Phys. Rev. D **49**, 5746 (1994).
- [28] G. M. Frichter, D. W. McKay, and J. P. Ralston, Phys. Rev. Lett. **74**, 1508 (1995).
- [29] A. Capella, A. B. Kaidalov, C. Merino, and J. Tran Thanh Van, Phys. Lett. B **337**, 358 (1994); A. B. Kaidalov, C. Merino, and D. Pertermann, Eur. Phys. J. C **20**, 301 (2001); P. Desgrolard, L. L. Jenkovszky, and F. Paccanoni, Eur. Phys. J. C **7**, 655 (1999); V. I. Vovk, A. V. Kotikov, and S. I. Maximov, Theor. Math. Phys. **84**, 744 (1990); L. L. Jenkovszky, A. V. Kotikov, and F. Paccanoni, Sov. J. Nucl. Phys. **55**, 1224 (1992); JETP Lett. **58**, 163 (1993); Phys. Lett. B **314**, 421 (1993); A. V. Kotikov, S. I. Maximov, and I. S. Parobij, Theor. Math. Phys. **111**, 442 (1997).
- [30] A. D. Martin, W. S. Stirling, and R. G. Roberts, Phys. Lett. B **B387**, 419 (1996).
- [31] V. S. Fadin and L. N. Lipatov, Phys. Lett. B **429**, 127(1998); G. Camici and M. Ciafaloni, Phys. Lett. **B430**, 349 (1998); A. V. Kotikov and L. N. Lipatov, Nucl. Phys. B **582**, 19 (2000); **661**, 19 (2003).
- [32] G. Grunberg, Phys. Rev. D **29**, 2315 (1984); Phys. Lett. B **95**, 70 (1980).
- [33] Yu. L. Dokshitzer and D. V. Shirkov, Z. Phys. C **67**, 449 (1995); A. V. Kotikov, JETP Lett. **59**, 1 (1994); Phys. Lett. B **338**, 349 (1994); W. K. Wong, Phys. Rev. D **54**, 1094 (1996).
- [34] S. J. Brodsky, V. S. Fadin, V. T. Kim *et al.*, JETP. Lett. **70**, 155 (1999); M. Ciafaloni, D.

- Colferai, and G. P. Salam, Phys. Rev. D **60**, 114036 (1999); JHEP **07**, 054 (2000); R. S. Thorne, Phys. Lett. B **474**, 372 (2000); Phys. Rev. D **60**, 054031 (1999); **64**, 074005 (2001); G. Altarelli, R. D. Ball, and S. Forte, Nucl. Phys. B **621**, 359 (2002).
- [35] Bo Andersson *et al.*, Eur. Phys. J. C **25**, 77 (2002).
- [36] A. V. Nesterenko, Phys. Rev. D **64**, 116009 (2001); Int. J. Mod. Phys. **A18**, 5475 (2003); A. V. Nesterenko and J. Papavassiliou, Phys. Rev. D **71**, 016009 (2005); J. Phys. G **32**, 1025 (2006); G. Cvetič, C. Valenzuela, and I. Schmidt, Nucl. Phys. Proc. Suppl. **164**, 308 (2007); G. Cvetič and C. Valenzuela, J. Phys. G **32**, L27 (2006); Phys. Rev. D **74**, 114030 (2006); Phys. Rev. D **77**, 074021 (2008); A. P. Bakulev, S. V. Mikhailov, and N. G. Stefanis, Phys. Rev. D **72**, 074014 (2005); Phys. Rev. D **75**, 056005 (2007); R. S. Pasechnik, D. V. Shirkov, and O. V. Teryaev, Phys. Rev. D **78**, 071902 (2008); R. S. Pasechnik, D. V. Shirkov, O. V. Teryaev, O. P. Solovtsova, and V. L. Khandramai, arXiv:0911.3297 [hep-ph].
- [37] G. Cvetič and C. Valenzuela, Braz. J. Phys. **38**, 371 (2008); A. P. Bakulev, S. V. Mikhailov, arXiv:0803.3013 [hep-ph]; N. G. Stefanis, arXiv:0902.4805 [hep-ph].
- [38] G. Cvetič, A.Yu. Illarionov, B.A. Kniehl, and A.V. Kotikov, Phys. Lett. **B679**, 350 (2009).
- [39] A. V. Kotikov, A. V. Lipatov, and N. P. Zotov, J. Exp. Theor. Phys. **101**, 811 (2005).

Figure captions

Fig. 1. $F_2(x, Q^2)$ as a function of x for different Q^2 bins. The experimental points are from H1 [1] (open points) and ZEUS [2] (solid points) at $Q^2 \geq 1.5 \text{ GeV}^2$. The solid curve represents the NLO fit. The dashed curve (hardly distinguishable from the solid one) represents the LO fit.

Fig. 2. $F_2(x, Q^2)$ as a function of x for different Q^2 bins. The experimental points are same as on Fig. 1. The solid curve represents the NLO fit. The dash-dotted curve represents the BFKL-motivated estimation for higher-twist corrections to $F_2(x, Q^2)$ (see [15]). The dashed curve is obtained from the fits at the NLO, when the renormalon contributions of higher-twist terms have been incorporated.

Fig. 3. $F_2(x, Q^2)$ as a function of x for different Q^2 bins. The experimental points are from H1 [1] (open points) and ZEUS [2] (solid points) at $Q^2 \geq 0.5 \text{ GeV}^2$. The solid curve represents the NLO fit. The dashed curve is from the fits at the NLO with the renormalon contributions of higher-twist terms incorporated. The dash-dotted curve (hardly distinguishable from the dashed one) represents the LO fit with the renormalon contributions of higher-twist terms incorporated.

Fig. 4. The values of effective slope $\lambda_{F_2}^{\text{eff}}$ as a function of Q^2 for $x = 10^{-3}$. The experimental points are from H1 [4, 5] (open points) and ZEUS [3] (solid points). The solid curve represents the NLO fit. The dash-dotted and lower dashed curves represent the NLO fits with “frozen” and analytic coupling constants, respectively. The top dashed line represents the fit from [4].

Figure 5. The values of effective slope $\lambda_{F_2}^{\text{eff}}$ as a function of Q^2 . The experimental points are same as on Fig. 4. The dashed line represents the fit from [4]. The solid curves represent the NLO fits with “frozen” coupling constant at $x = 10^{-2}$ and $x = 10^{-5}$.

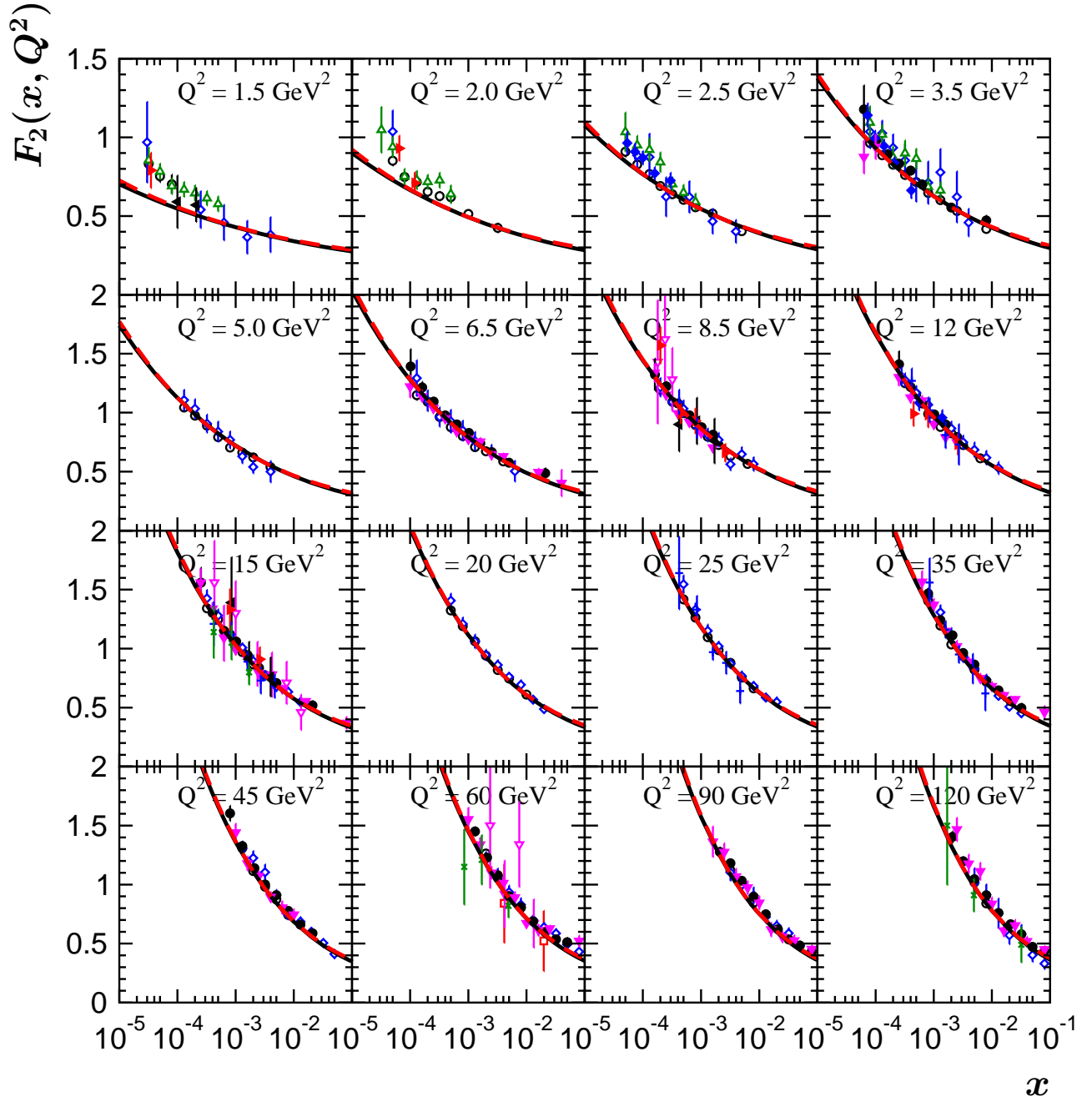


FIG. 1: $F_2(x, Q^2)$ as a function of x for different Q^2 bins. The experimental points are from H1 [1] (open points) and ZEUS [2] (solid points) at $Q^2 \geq 1.5 \text{ GeV}^2$. The solid curve represents the NLO fit. The dashed curve (hardly distinguishable from the solid one) represents the LO fit.

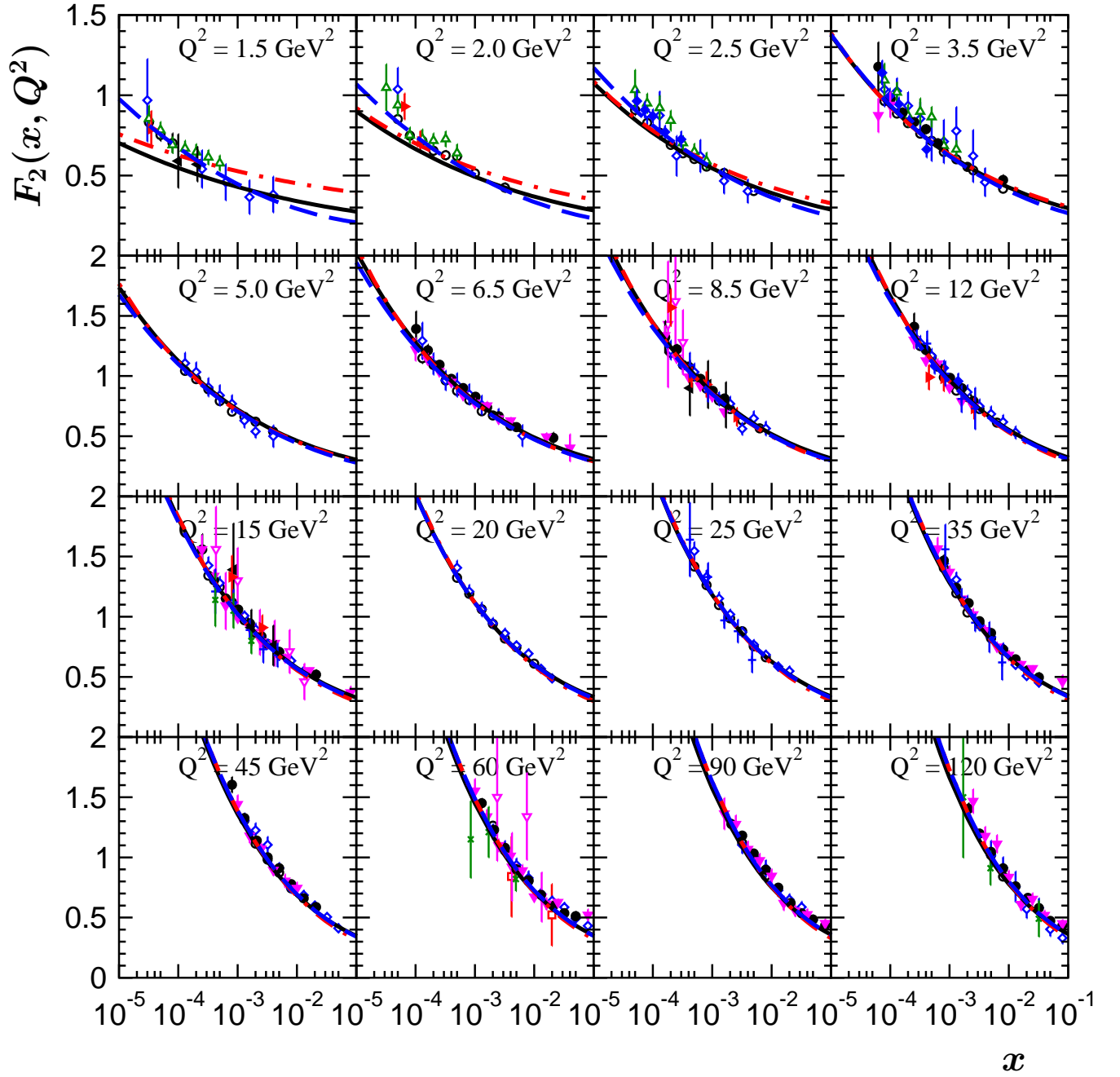


FIG. 2: $F_2(x, Q^2)$ as a function of x for different Q^2 bins. The experimental points are same as on Fig. 1. The solid curve represents the NLO fit. The dash-dotted curve represents the BFKL-motivated estimation for higher-twist corrections to $F_2(x, Q^2)$ (see [15]). The dashed curve is obtained from the fits at the NLO, when the renormalon contributions of higher-twist terms have been incorporated.

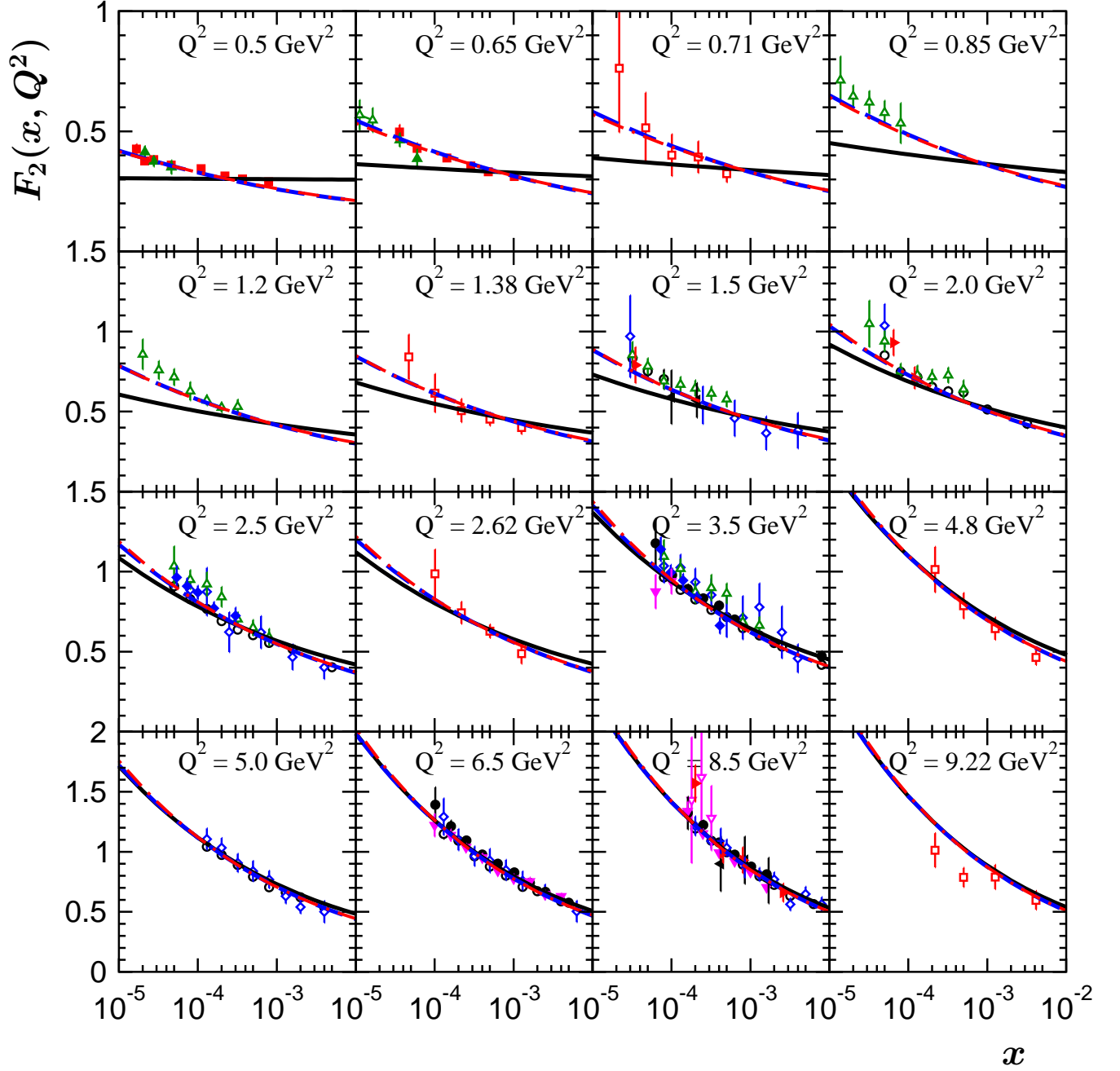


FIG. 3: $F_2(x, Q^2)$ as a function of x for different Q^2 bins. The experimental points are from H1 [1] (open points) and ZEUS [2] (solid points) at $Q^2 \geq 0.5 \text{ GeV}^2$. The solid curve represents the NLO fit. The dashed curve is from the fits at the NLO with the renormalon contributions of higher-twist terms incorporated. The dash-dotted curve (hardly distinguishable from the dashed one) represents the LO fit with the renormalon contributions of higher-twist terms incorporated.

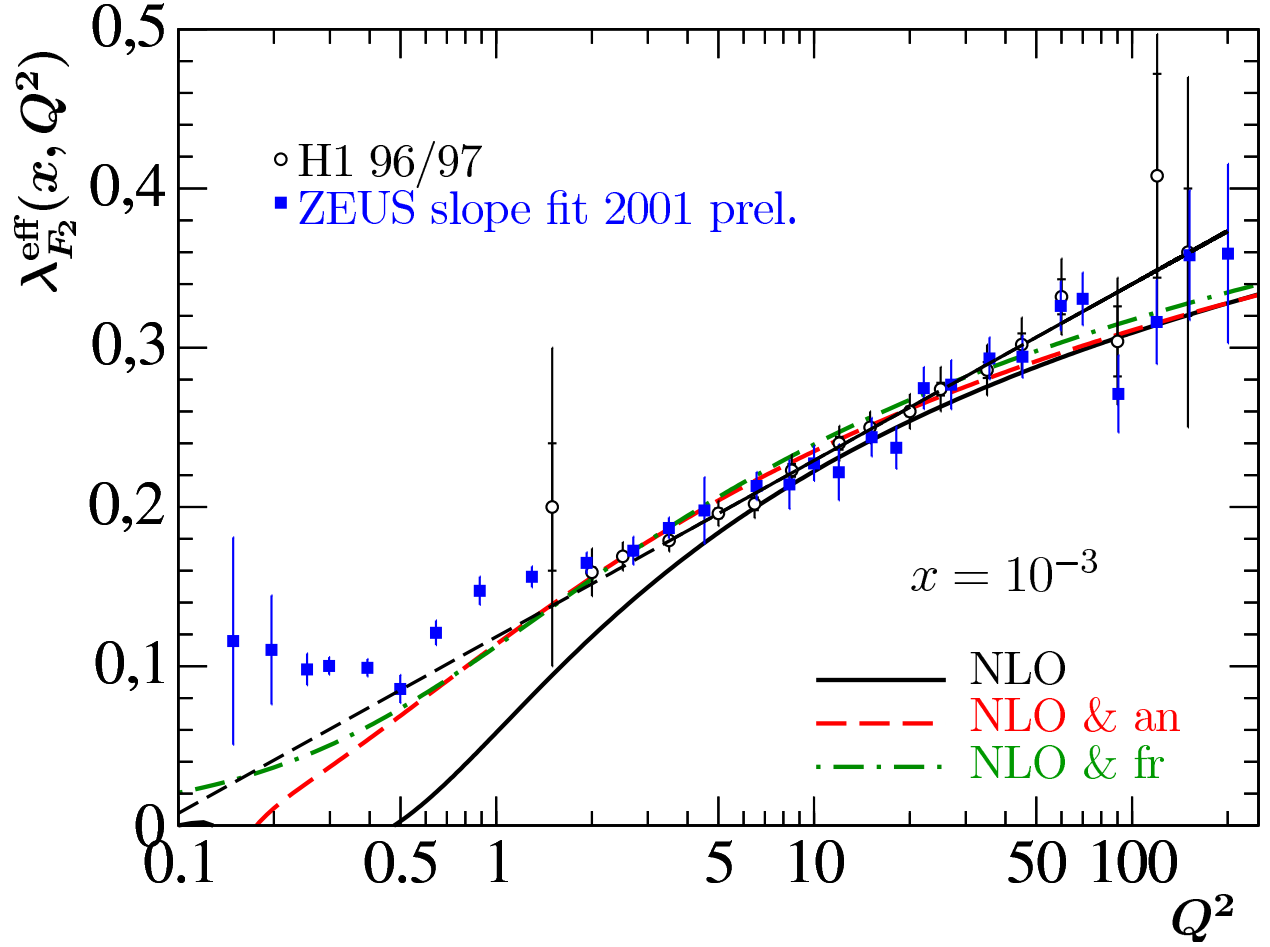


FIG. 4: The values of effective slope $\lambda_{F_2}^{\text{eff}}$ as a function of Q^2 for $x = 10^{-3}$. The experimental points are from H1 [4, 5] (open points) and ZEUS [3] (solid points). The solid curve represents the NLO fit. The dash-dotted and lower dashed curves represent the NLO fits with “frozen” and analytic coupling constants, respectively. The top dashed line represents the fit from [4].

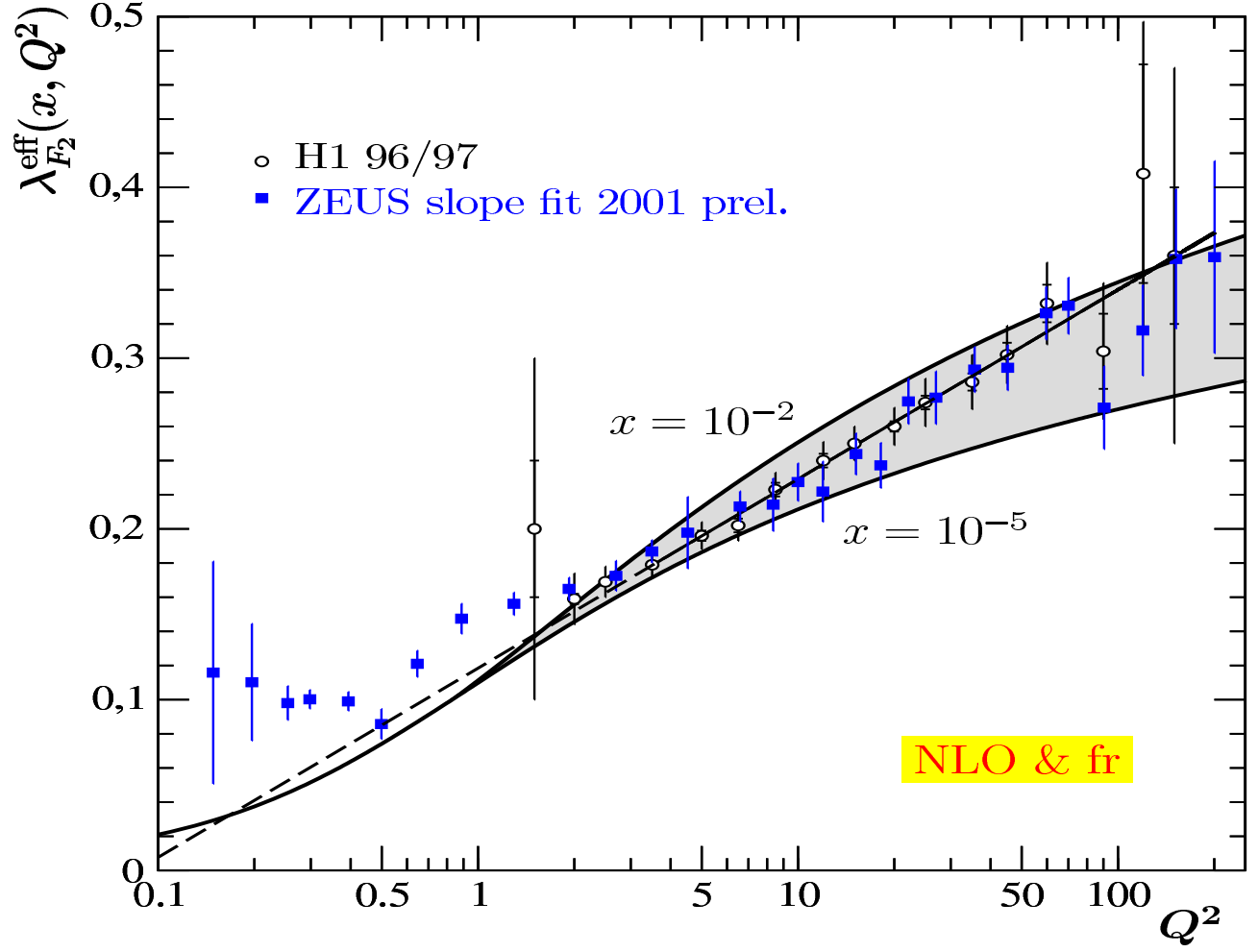


FIG. 5: The values of effective slope $\lambda_{F_2}^{\text{eff}}$ as a function of Q^2 . The experimental points are same as on Fig. 4. The dashed line represents the fit from [4]. The solid curves represent the NLO fits with “frozen” coupling constant at $x = 10^{-2}$ and $x = 10^{-5}$.